Electronic Supplementary Material (ESI) for Journal of Materials Chemistry A.

Electronic Supporting Information

Metallated Azo-Naphthalene Diimide based Redox Active Porous Organic Polymer as Efficient Water Oxidation Electrocatalyst

Sajad Ahmad Bhat, Chayanika Das, and Tapas Kumar Maji*

Experimental Section

Materials

All the reagents employed were commercially available and used as provided without further purification. Cobalt acetate tetrahydrate [$Co(OAc)_2 \cdot 4H_2O$], 1,4,5,8-naphthalenetetracarboxylic anhydride, paraphenylene diamine and benzidine was obtained from Sigma Aldrich Chemicals. Phloroglucinol was purchased from Spectrochem. All other reagents and solvents were purchased from commercial sources and used as supplied. naphthalenediimide diamine (NDI-diamine) was synthesised following the literature procedure. (*Chem. Sci.* 2015, 2614).

Synthesis of naphthalenediimide diamine (NDI diamine)

1,4,5,8-naphthalenetetracarboxylic dianhydride (0.34 g, 1.3 mmol) and 1,4-diaminobenzene (0.34 g, 3.2 mmol) were suspended in 12 mL of dry DMF, in a 30 mL MW (microwave) vial and sonicated for 30 min. Triethylamine (0.86 mL, 65 mmol) was added and the reaction mixture was heated to reflux for 15 min at 140 ± 5 °C under microwave irradiation. The resulting mixture was filtered and the residue was washed with copious amounts of water, acetone and then chloroform. NDI **1** was isolated as a brown powder (1.55 g, 93%) and was used without further purification. ^1H NMR (400 MHz: [D6]-DMSO) $\delta = 8.75$ (4H, s, H4), 7.01 (4H, d, $J = 8.5$ Hz, H3) 6.66 (4H, d, $J = 8.5$ Hz, H2) 5.29 (4H, s, H1).

Synthesis of NDI-PG Polymer

0.53 g (1.2 mmol) of naphthalenediimide diamine (NDI diamine) was taken in flat bottomed 250 mL flask and charged with 100 mL of distilled water and 1.4 mL of 35% hydrochloric acid. The mixture was stirred for 15-20 minutes at 0-5 °C and 30 mL of aqueous solution of sodium nitrite (0.17 g, 2.45 mmol) was added dropwise. The solution was stirred for further 30 minutes to make amino groups to convert completely to diazonium salts. The solution was neutralized with dilute solution of sodium carbonate. The mixture was then added in portions to an aqueous solution of trihydroxybenzene (0.1 g, 0.8 mmol) and Na_2CO_3 (0.25 g, 2.38 mmol) at 0~ 5 °C. During addition, colour of solution changed to brick red and was further stirred overnight. The solid sample was separated from the mixture by filtration and was washed with methanol, THF, DMF, water and further purification of the sample was carried out by soxhlet extraction with water, THF, acetone and DMF. The product was dried in a vaccum at 100 °C and isolated as brick red solid (yield: 0.52 g).

Loading of Co^{II} into -NDI-PG Polymer

50 mg of as synthesized **NDI-PG** Polymer (in 10 mL of ethanol) was treated with calculated amount of $Co(OAc)_2 \cdot 4H_2O$ (50 mg, 25 mg, 12.5 mg) dissolved in 10 mL of ethanol and 0.5 mL 0f triethylamine. After refluxing for 10 hours, the mixture was filtered and washed with copious amount of methanol and dried under vacuum overnight at 100 °C. The 10%, 8% and 7% cobalt loadings were obtained as analysed through ICP analysis. The highest cobalt loading was obtained on using 50 mg of $Co(OAc)_2 \cdot 4H_2O$ and loading of the cobalt content was found to remain constant after treatment with more than 50 mg of $Co(OAc)_2 \cdot 4H_2O$.

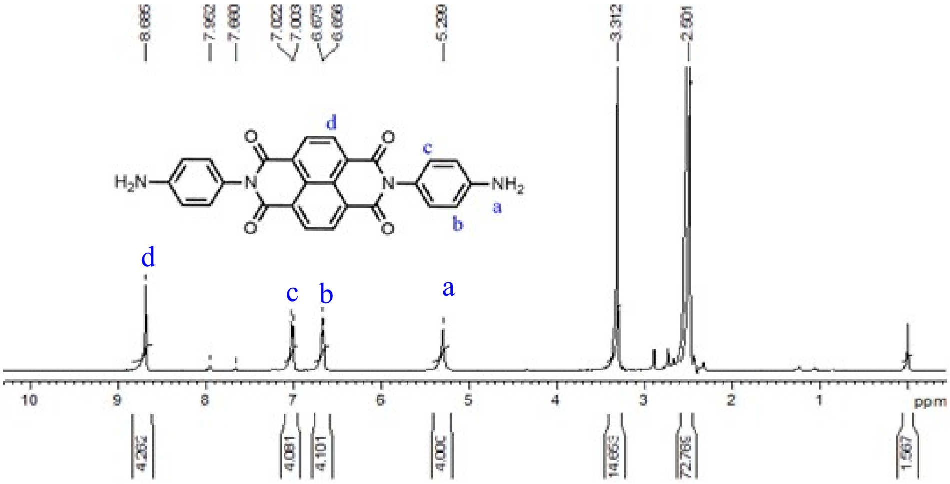

Figure S1. ^1H NMR spectrum of naphthalenediimide diamine in d6-DMSO.

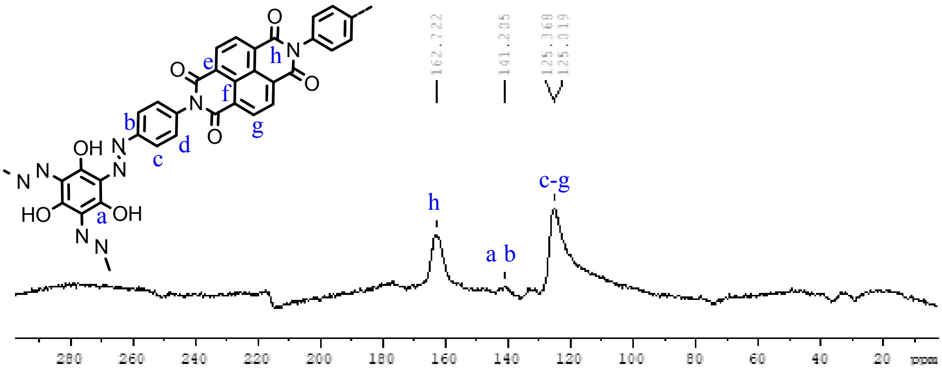

Figure S2. Solid-state ^{13}C-CP/MAS NMR spectrum of **NDI-PG** Polymer.

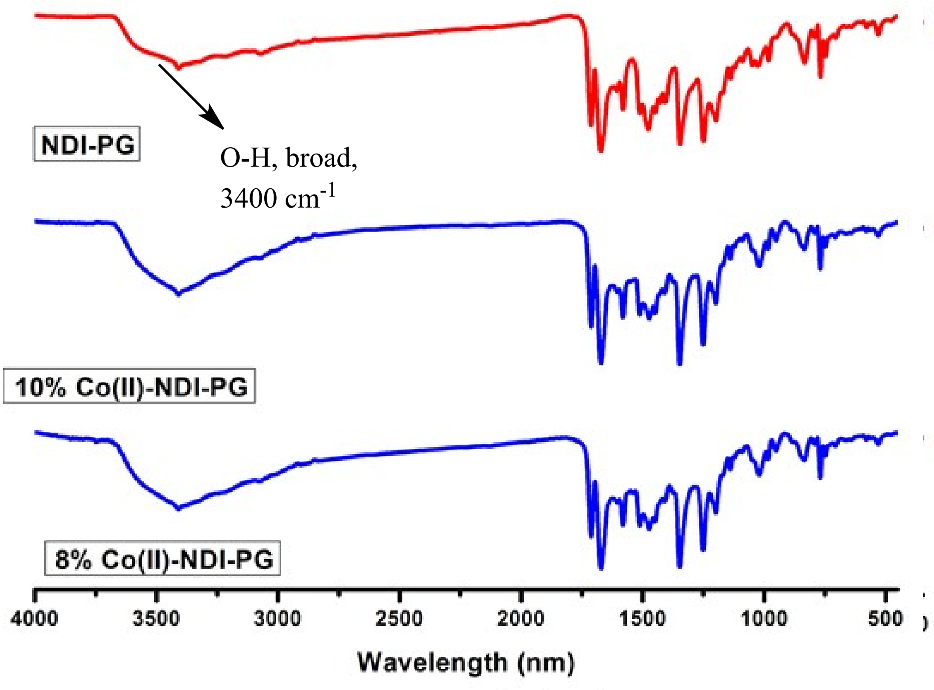

Figure S3. FT-IR spectra of the **NDI-PG,** 10% **Co^{II}-NDI-PG** and 8% **Co^{II}-NDI-PG**. The spectra were recorded using KBr pellets.

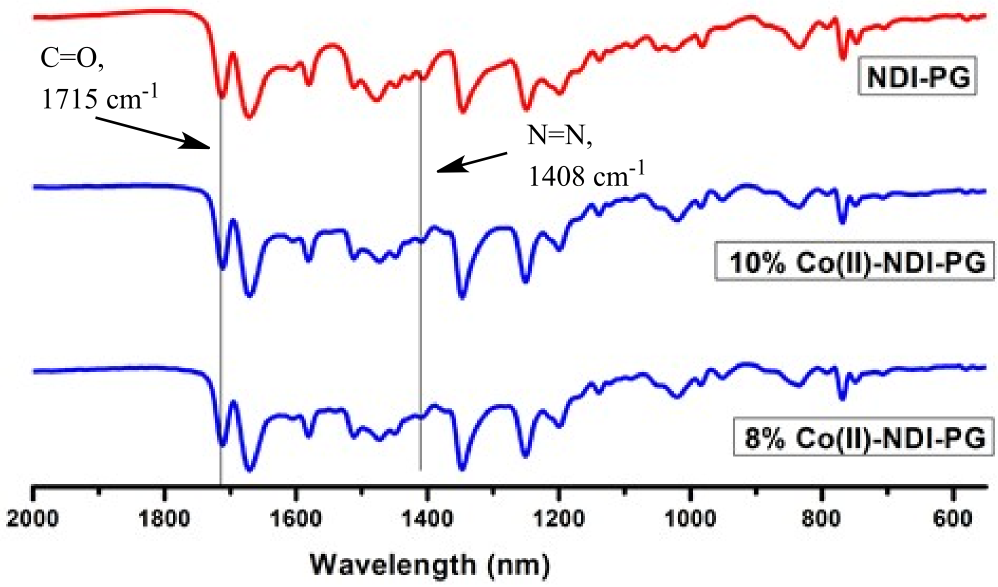

Figure S4. FT-IR spectra (region 500-2000 cm^{-1}) of the **NDI-PG,** 10% **Co^{II}-NDI-PG** and 8% **Co^{II}-NDI-PG**. The spectra were recorded using KBr pellets.

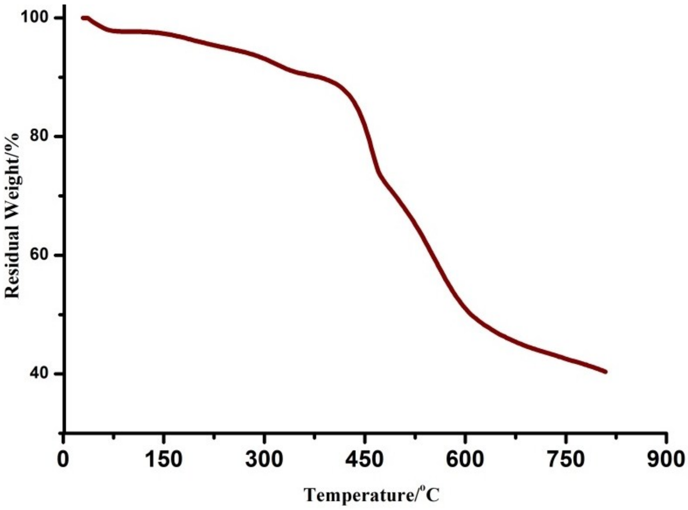

Figure S5. Thermogravimetric analysis (TGA) of **NDI-PG** under air atmosphere.

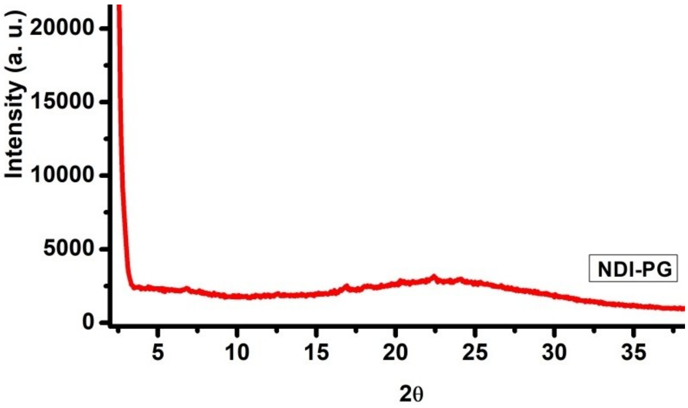

Figure S6. Powder X-ray Diffraction (PXRD) of **NDI-PG**.

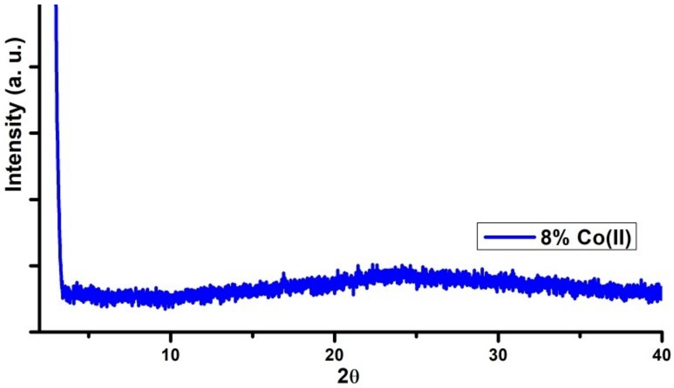

Figure S7. Powder X-ray Diffraction (PXRD) of 8% **Co^{II}-NDI-PG.**

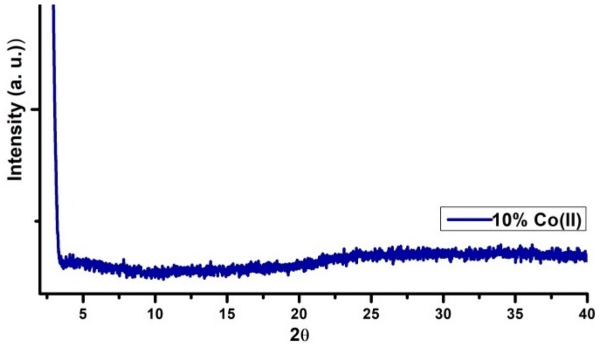

Figure S8. Powder X-ray Diffraction (PXRD) of **10% Co^{II}-NDI-PG.**

The powder X-ray diffraction patterns of **NDI-PG**, 8% **Co^{II}-NDI-PG** and 10% **Co^{II}-NDI-PG** are shown in Figures S6-S8. The PXRD patterns of these samples show a characteristic broad peak near 20-25°, like most of amorphous polymers indicating they are in amorphous nature. So the spatial arrangement of polymer molecules in the powder form is not ordered.

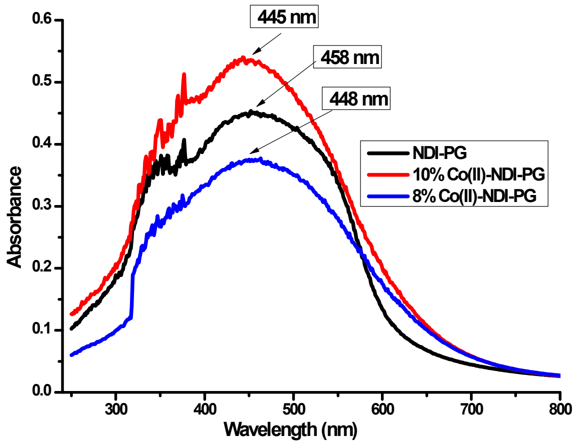

Figure S9. Solid UV/Vis spectra of **NDI-PG,** 10% **Co^{II}-NDI-PG** and 8% **Co^{II}-NDI-PG.**

The planar electron deficient π-conjugated NDI core within the porous polymer facilitates electron delocalization and favours π-π stacking. The broad band in the absorption spectrum is probably due to delocalized π-electron cloud of the NDI-PG.

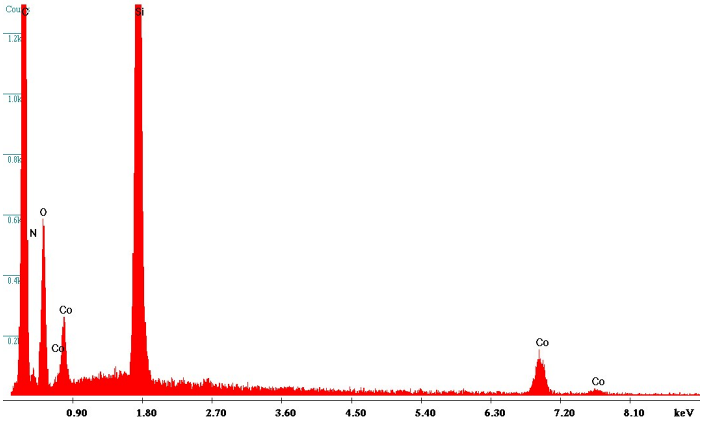

Figure S10: EDX spectra of 8% **Co^{II}-NDI-PG**.

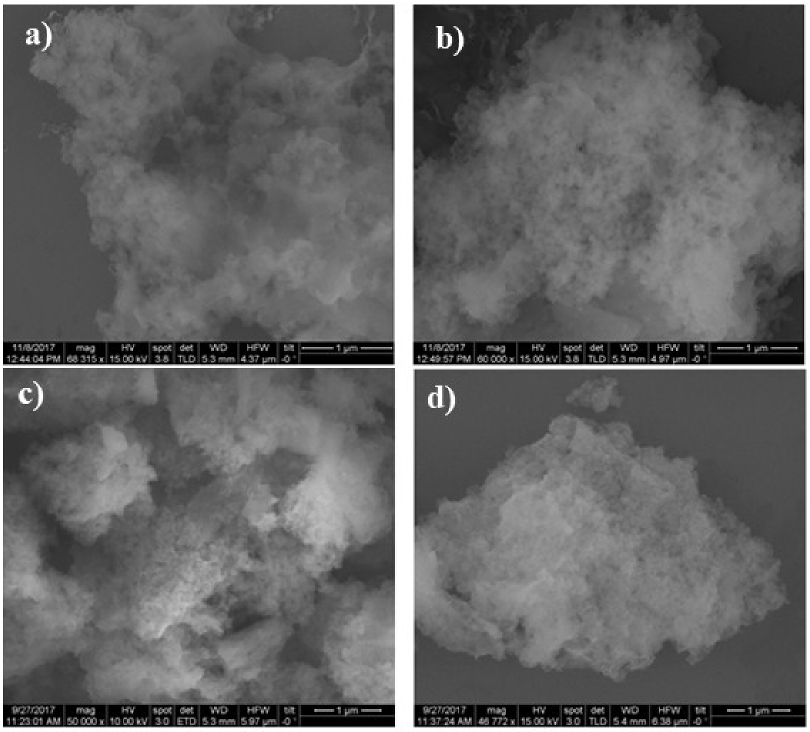

Figure S11: FESEM of a,b) **NDI-PG** and c,d) 8 % **Co^{II}-NDI-PG.**

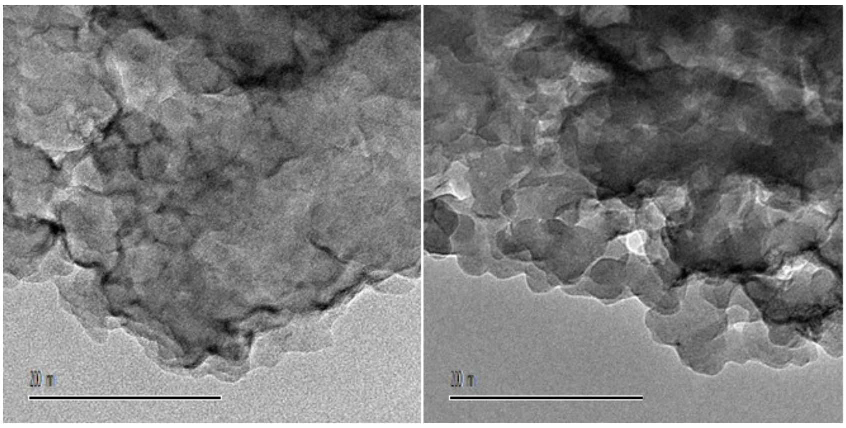

Figure S12: TEM images of **Co^{II}-NDI-PG**.

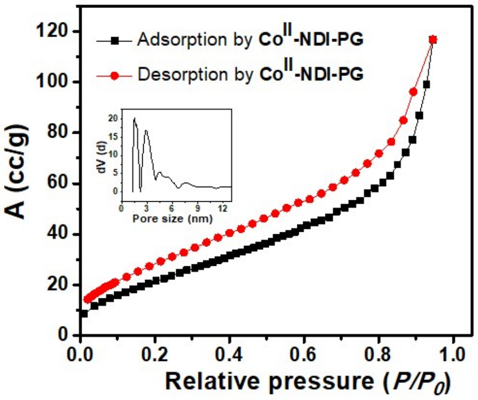

Figure S13: N_2 adsorption of 8 % **Co^{II}-NDI-PG** at 77 K and corresponding pore size distribution (inset).

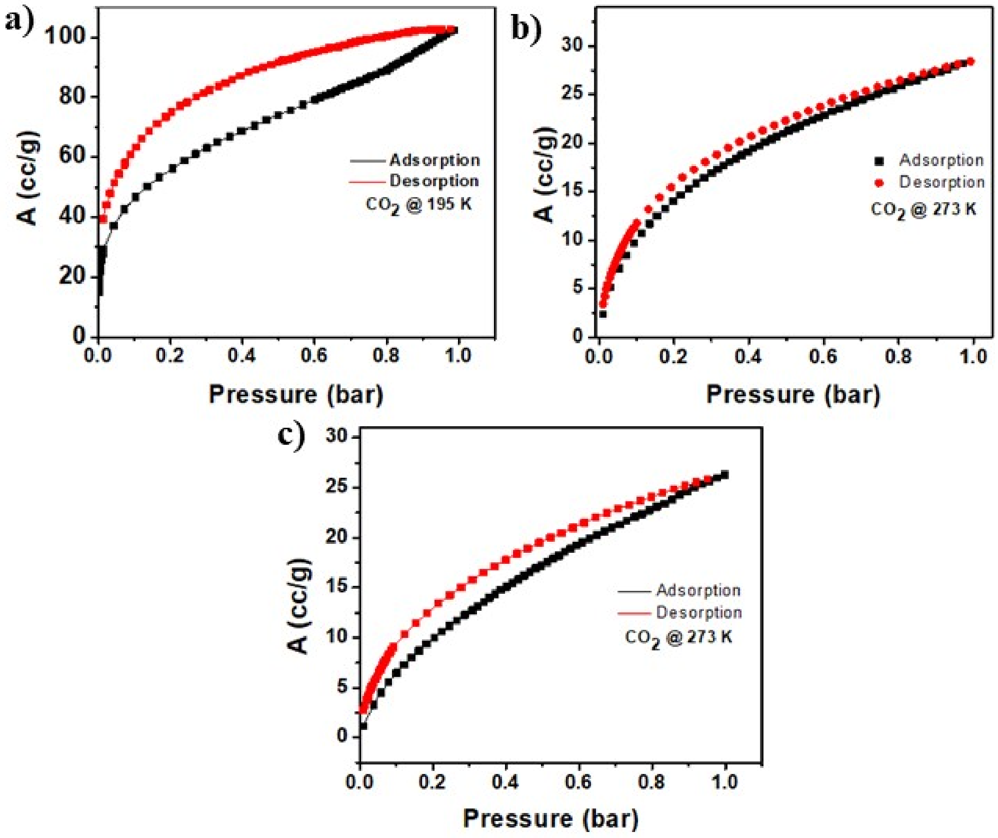

Figure S14: a,b) CO_2 adsorption of **NDI-PG** at 195 K and c) CO_2 adsorption of 8 % **Co^{II}-NDI-PG** at 273 K.

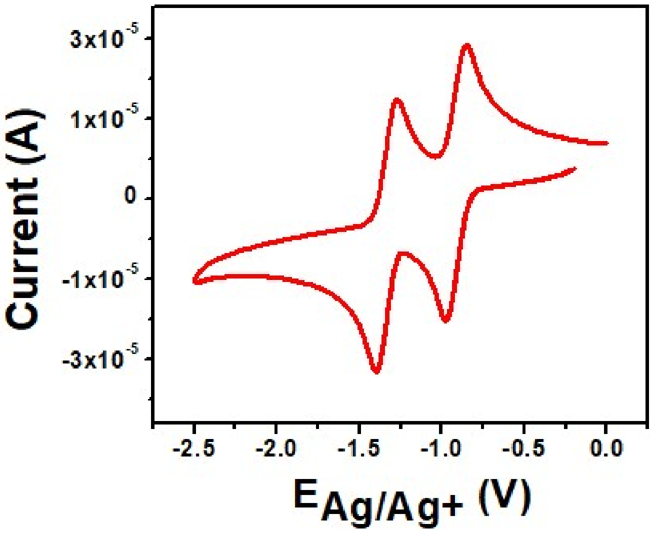

Figure S15: Cyclic voltammogram of **NDI-DA** (10 mVs^{-1}, DMSO, 0.1 M in $TBAPF_6$ supporting electrolyte.

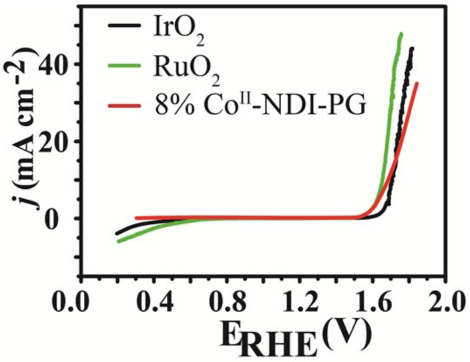

Figure S16: LSV comparing the OER activities of IrO_2, RuO_2 and 8% **Co^{II}-NDI-PG.**

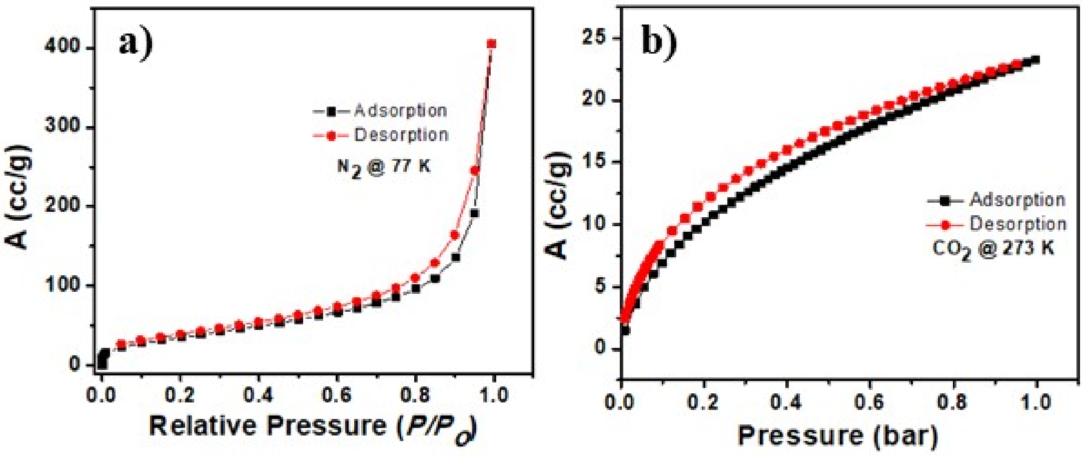

Figure S17: a) N_2 adsorption isotherm at 77 K and b) CO_2 adsorption isotherm at 273 K of **BD-PG.**

Electrochemical Impedance spectroscopy

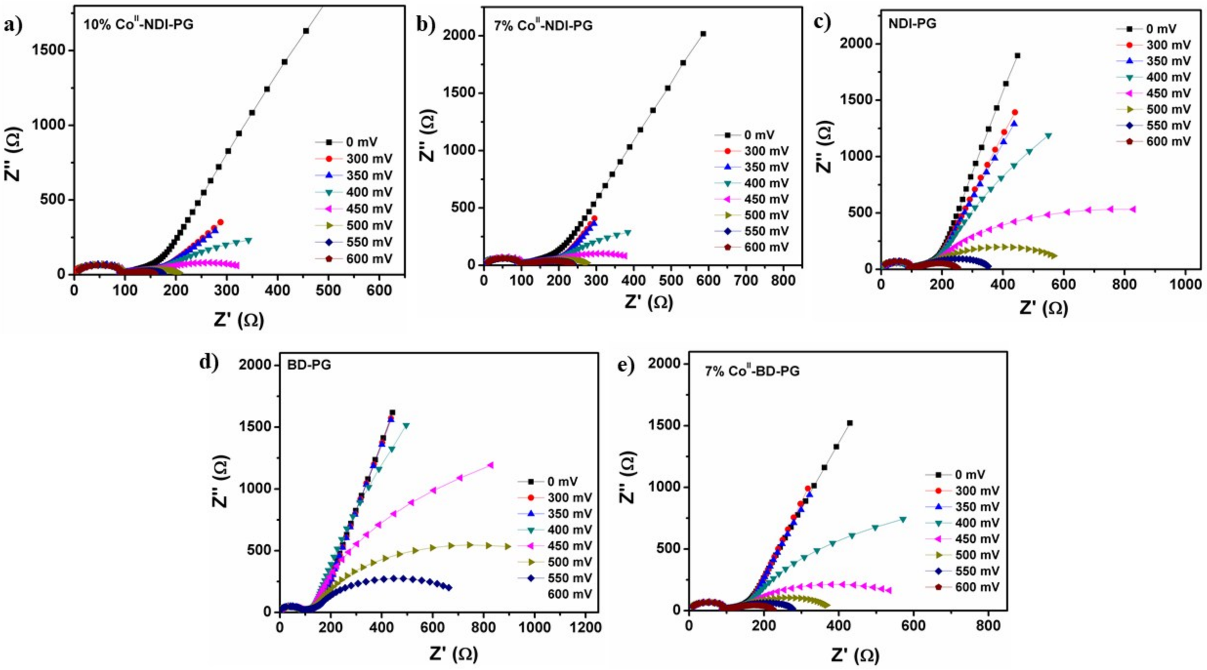

Figure 18: Impedance recorded at various overpotentials for a) 10% **Co^{II}-NDI-PG**, b) 7% **Co^{II}-NDI-PG**, c) **NDI-PG**, d) **BD-PG** and e) 10% **Co^{II}-BD-PG**.

Roughness Factor (RF) and Turn Over Frequency (TOF)

$$RF = \frac{Electrochemical\ Active\ Surface\ Area\ (EASA)}{Geometrical\ Surafce\ Area\ (GSA)}$$

Where,

$$EASA = \frac{C_{dl}}{C_s}$$

RF before 500 cycles of LSV: CV for both the bare GCE and the electrocatalyst coated GC were recorded in the capacitive potential region and the slopes of the corresponding current vs scanrate plots gives the C_{dl} and C_s.

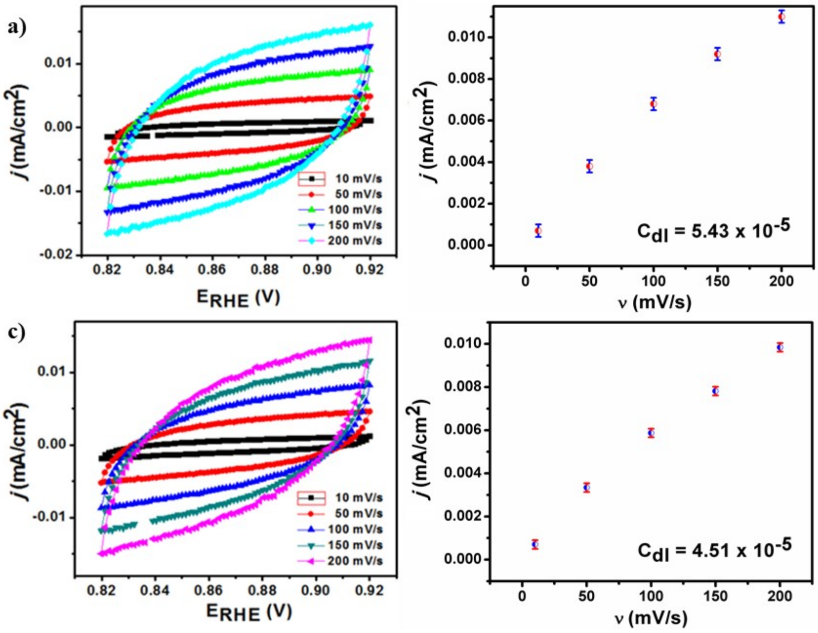

Figure S19: a, b) CV at the capacitance potential region at various scan rates and the corresponding current-scan rate plot for bare GCE, respectively; c,d) CV at the capacitance potential region at various scan rates and the corresponding current-scan rate plot for 8% **Co^{II}-NDI-PG** coated GCE before 500 cycles of LSV respectively.

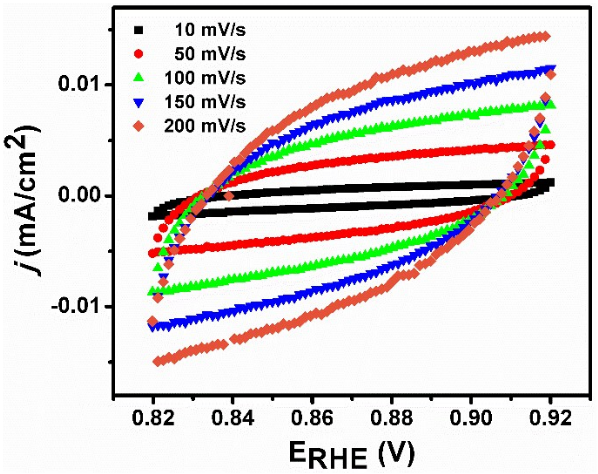

Figure S20: CV at the capacitance potential region at various scan rates for 8% **Co^{II}-NDI-PG** coated GCE after 500 cycles of LSV.

Calculation of TOF:

The TOF is calculated by the formula given below

$$TOF = \frac{i}{4\ x\ F\ x\ RF\ x\ m}$$

Where, F = Faraday constant, m = no of moles of Co, this is calculated from the slope of current-scan rate plot of Co-peak (Figure S20) from the formula given below:

$$m = \frac{4RT\ x\ slope}{n^2F^2}$$

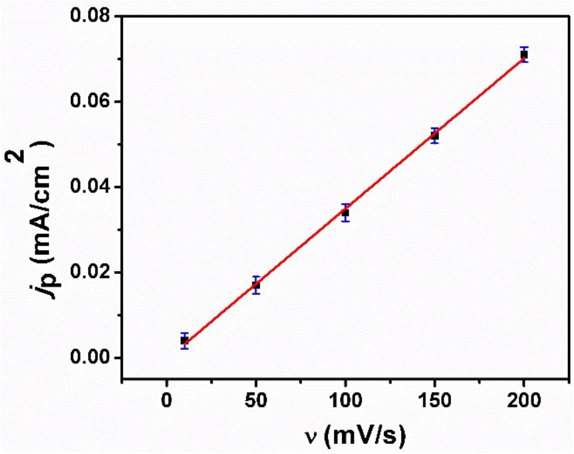

Figure S21: Co $^{II/III}$ peak current vs scan rate.

Table S1: R_{film} and R_p values for all samples at various overpotentials.

Sample	0 mV		300 mV		350 mV		400 mV		450 mV		500 mV		550 mV		600 mV	
	R_{film}	R_p	R_{film}	R_p	R_{film}	R_p	R_{film}	R_p	R_{film}	R_p	R_{film}	R_p	R_{film}	R_p	R_{film}	R_p
10% Co-NDI-PG	90	4000	90	1200	90	800	90	650	90	380	90	210	88	176	88	160
8% Co-NDI-PG	82	4000	81	1100	81	1100	81	600	80	370	80	220	80	171	79	146
7% Co-NDI-PG	91	5500	90	1800	90	1700	90	1000	90	440	91	280	90	240	90	240
NDI-PG	95	5500	95	2500	95	2500	95	1800	95	650	95	390	95	290	95	225
7% Co-BD-PG	96	8000	96	3500	96	3000	96	2800	93	2500	93	650	93	360	93	260
BD-PG	100	5800	100	4500	100	3700	100	3300	100	3000	100	1400	100	900	100	630

Faradaic Efficiency (ε)

The faradaic efficiency (ε) of 8% **Co^{II}-NDI-PG** for the oxygen evolution electrocatalysis was determined by rotating ring disk electrode (RRDE) method.[1-3] The Ring potential was maintained at 1.2 V with respect to RHE and the disk current was varied from 1-15 mA/cm^2 in steps and the corresponding disk voltage was recorded. The ε was calculated by the following equation:

$$\varepsilon = \frac{2I_r}{NI_d}$$

Where I_r is the ring current, I_d is the disk current and N is the collection efficiency of the RRDE.

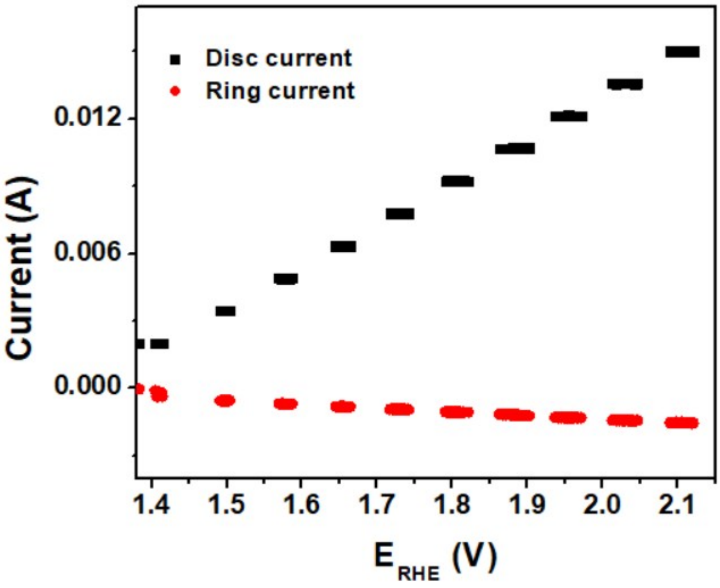

Figure S22: Ring current and disk current recorded for 8% **Co^{II}-NDI-PG** for the calculation of faradaic efficiency.

Reference:

1 H. B. Aiyappa, J. Thote, D. B. Shinde, R. Banerjee and S. Kurungot, *Chem. Mater.*, 2016, **28**, 4375.

2 C. C. L. McCrory, S. Jung, J. C. Peters and T. F. Jaramillo, *J. Am. Chem. Soc.*, 2013, **135**, 16977.

3 A. T. Swesi, J. Masud and M. Nath, *Energy Environ. Sci.,* 2016, **9**, 1771.